

ADAPTIVE VIRTUAL ELEMENTS BASED ON HYBRIDIZED, RELIABLE, AND EFFICIENT FLUX RECONSTRUCTIONS

FRANCO DASSI, JOSCHA GEDICKE, AND LORENZO MASCOTTO

ABSTRACT. We present two a posteriori error estimators for the virtual element method (VEM) based on global and local flux reconstruction in the spirit of [6]. The proposed error estimators are reliable and efficient for the h -, p -, and hp -versions of the VEM. This solves a partial limitation of our former approach in [7], which was based on solving local nonhybridized mixed problems. Differently from the finite element setting, the proof of the efficiency turns out to be simpler, as the flux reconstruction in the VEM does not require the existence of polynomial, stable, divergence right-inverse operators. Rather, we only need to construct right-inverse operators in virtual element spaces, exploiting only the implicit definition of virtual element functions. The theoretical results are validated by some numerical experiments on a benchmark problem.

AMS subject classification: 65N12, 65N30, 65N5

Keywords: virtual element method, hybridized methods, equilibrated fluxes, hp -adaptivity, polygonal meshes

1. INTRODUCTION

In [7], we analyzed certain error estimators for the virtual element method (VEM) [3], based on global and local flux reconstruction via mixed problems. To the aim, we mainly followed the finite element (FE) and discontinuous Galerkin (dG) approach of [9] and realized that the VEM contains too many variational crimes to allow for a localized, efficient error estimator with such an approach. In this paper, we undertake a slightly different path, i.e., we design error estimators by means of flux reconstruction via hybridized mixed methods. Notably, we adapt the finite element framework [6] to the virtual element one, which is based on polygonal meshes that are more suited for mesh adaptation as they naturally handle hanging nodes.

We shall design two error estimators based on global and local flux reconstructions, and prove their reliability and efficiency for the h -, p -, and hp versions of the VEM. In both cases, the proof of the efficiency turns out to be more straightforward than the finite element one. Indeed, when using virtual elements, the existence of a polynomial, divergence right-inverse operator, see [6, Theorem 5 and Conjecture 6], is not required.

As a pivot result, we also prove the existence of a stabilization term for mixed virtual elements, with stability constants having explicit dependence on the degree of accuracy of the method. Furthermore, we discuss in details the flux reconstruction, well posedness of the hybridized mixed VEM; see also [8] for the hybridization of the mixed VEM in linear elasticity.

Notation. We consider standard notation for Sobolev spaces. Given a domain D , $H^s(D)$ denotes the standard Sobolev space of order s , which we endow with the standard inner product $(\cdot, \cdot)_{s,D}$, norm $\|\cdot\|_{s,D}$, and seminorm $|\cdot|_{s,D}$. Fractional and negative Sobolev spaces are defined via interpolation and duality, respectively. Recall the definition of standard differential equations in two dimensions: given $v : \mathbb{R}^2 \rightarrow \mathbb{R}$ and $\boldsymbol{\tau} = (\boldsymbol{\tau}_1, \boldsymbol{\tau}_2) : \mathbb{R}^2 \rightarrow \mathbb{R}^2$,

$$\operatorname{div} \boldsymbol{\tau} := \partial_x \boldsymbol{\tau}_1 + \partial_y \boldsymbol{\tau}_2, \quad \operatorname{rot} \boldsymbol{\tau} := \partial_y \boldsymbol{\tau}_1 - \partial_x \boldsymbol{\tau}_2, \quad \operatorname{curl} v := (\partial_y v; -\partial_x v).$$

In light of the above definitions, we also introduce the spaces

$$H(\operatorname{div}, D) := \{\boldsymbol{\tau} \in [L^2(D)]^2 \mid \operatorname{div} \boldsymbol{\tau} \in L^2(D)\}, \quad H(\operatorname{rot}, D) := \{\boldsymbol{\tau} \in [L^2(D)]^2 \mid \operatorname{rot} \boldsymbol{\tau} \in L^2(D)\}.$$

Given two positive quantities a and b , we shall write “ $a \lesssim b$ ” instead of “there exists a positive constant C , independent of the discretization parameters, such that $a \leq C b$ ”.

The model problem. Given a polygonal domain $\Omega \subset \mathbb{R}^2$ and $f \in L^2(\Omega)$, we consider the Poisson problem: find \tilde{u} such that

$$\begin{cases} -\Delta \tilde{u} = f & \text{in } \Omega \\ \tilde{u} = 0 & \text{on } \partial\Omega, \end{cases} \quad (1)$$

where $\partial\Omega$ denotes the boundary of Ω .

The weak formulation of (1) reads

$$\begin{cases} \text{find } \tilde{u} \in \tilde{V} \text{ such that} \\ \tilde{a}(\tilde{u}, \tilde{v}) = (f, \tilde{v})_{0,\Omega} \quad \forall \tilde{v} \in \tilde{V}, \end{cases} \quad (2)$$

where we have set

$$\tilde{V} := H_0^1(\Omega), \quad \tilde{a}(\tilde{u}, \tilde{v}) := (\nabla \tilde{u}, \nabla \tilde{v})_{0,\Omega} \quad \forall \tilde{u}, \tilde{v} \in \tilde{V}.$$

Problem (2) is well posed thanks to the Lax-Milgram lemma.

Mesh assumptions. We employ standard notation for polygonal meshes. More precisely, we consider sequences $\{\mathcal{T}_n\}_{n \in \mathbb{N}}$ of polygonal meshes with straight edges. Hanging nodes are naturally incorporated in such meshes. Given a mesh \mathcal{T}_n , we denote its set of edges and vertices by \mathcal{E}_n and \mathcal{V}_n . We split \mathcal{E}_n into the set of boundary and internal edges as follows:

$$\mathcal{E}_n^D := \{e \in \mathcal{E}_n \mid e \subset \partial\Omega\}, \quad \mathcal{E}_n^I := \mathcal{E}_n \setminus \mathcal{E}_n^D.$$

With each element $K \in \mathcal{T}_n$, we associate its diameter h_K , the outward pointing unit normal vector \mathbf{n}_K , its centroid \mathbf{x}_K , and its set of edges \mathcal{E}^K and vertices \mathcal{V}^K . Moreover, we associate with each edge $e \in \mathcal{E}_n$ its length h_e and any of the two unit normal vectors \mathbf{n}_e .

We consider standard properties for the sequence of meshes [3]: there exist two positive constants γ and $\tilde{\gamma}$, such that, for all $n \in \mathbb{N}$,

(A1) every $K \in \mathcal{T}_n$ is star-shaped with respect to a ball B with radius $r_B \geq \gamma h_K$;

(A2) given $K \in \mathcal{T}_n$, for every of its edges $e \in \mathcal{E}^K$, $h_K \leq \tilde{\gamma} h_e$.

Associated with each mesh \mathcal{T}_n and $p \in \mathbb{N}$, we define standard broken polynomial and Sobolev spaces:

$$\mathbb{P}_p(\mathcal{T}_n) := \{q_p \in L^2(\Omega) \mid q_p|_K \in \mathbb{P}_p(K) \forall K \in \mathcal{T}_n\};$$

$$H^1(\mathcal{T}_n) := \{v \in L^2(\Omega) \mid v|_K \in H^1(K) \forall K \in \mathcal{T}_n\};$$

$$H(\text{div}, \mathcal{T}_n) := \{\boldsymbol{\tau} \in [L^2(\Omega)]^2 \mid \boldsymbol{\tau}|_K \in H(\text{div}, \Omega)\}.$$

The first and second spaces can be generalized to the corresponding vector spaces.

Henceforth, for ease of presentation, we assume that $f \in \mathbb{P}_{p-1}(\mathcal{T}_n)$. Moreover, throughout the paper, we assume a uniform distribution of the polynomial degree p for the sake of presentation. The general case involving nonuniform distributions of polynomial degrees is a trivial generalization.

Structure of the paper. In Section 2, we review the hybridized global and local flux reconstruction in the finite element setting. After describing virtual elements for the primal and the hybridized mixed formulations in Section 3, we design and analyze the hybridized global and local flux reconstructions in the virtual element setting in Section 4. Notably, we introduce a reliable and efficient error estimator. Section 5 devotes to presenting numerical experiments validating the theoretical predictions. Finally, we state conclusions in Section 6

2. HYBRIDIZED GLOBAL/LOCAL FLUX RECONSTRUCTION IN THE FINITE ELEMENT SETTING

Here, we briefly recall the approach of [6] providing p robust, reliable and efficient error estimators on simplicial and Cartesian meshes for the finite element method. This will pave the way to design reliable and efficient error estimators for the virtual element method.

Let \mathcal{T}_n be a decomposition of Ω into triangles. We consider the standard finite element approximation of (2):

$$\begin{cases} \text{find } \tilde{u}_p \in \tilde{V}_p \text{ such that} \\ \tilde{a}(\tilde{u}_p, \tilde{v}_p) = (f, \tilde{v}_p)_{0,\Omega} \quad \forall \tilde{v}_p \in \tilde{V}_p, \end{cases} \quad (3)$$

where we have set

$$\tilde{V}_p := \mathbb{P}_p(\mathcal{T}_n) \cap H_0^1(\Omega).$$

We define a continuous residual $r \in [H_0^1(\Omega)]^*$ as

$$\langle r, \tilde{v} \rangle := (f, \tilde{v})_{0,\Omega} - \tilde{a}(\tilde{u}_p, \tilde{v}) \quad \forall \tilde{v} \in H_0^1(\Omega). \quad (4)$$

An integration by parts yields

$$\langle r, \tilde{v} \rangle := \sum_{K \in \mathcal{T}_n} (r^K, \tilde{v})_{0,K} + \sum_{e \in \mathcal{E}_n} (r^e, \tilde{v})_{0,e} \quad \forall \tilde{v} \in \tilde{V},$$

where we have introduced the bulk and internal edge residuals

$$r^K := f + \Delta \tilde{u}_p \in \mathbb{P}_{p-1}(K) \quad \forall K \in \mathcal{T}_n, \quad r^e := \llbracket \nabla \tilde{u}_p \rrbracket \in \mathbb{P}_{p-1}(e) \quad \forall e \in \mathcal{E}_n^I, \quad (5)$$

for the standard definition of the jump operator on an internal edge e :

$$\llbracket \boldsymbol{\tau} \rrbracket_e := \llbracket \boldsymbol{\tau} \rrbracket := \mathbf{n}_{K_1} \cdot \boldsymbol{\tau}_{K_1} + \mathbf{n}_{K_2} \cdot \boldsymbol{\tau}_{K_2}, \quad e \subset \overline{K_1} \cap \overline{K_2}, \quad \forall \boldsymbol{\tau}_p \in H(\operatorname{div}, \mathcal{T}_n).$$

The initial step towards the design of the hybridized flux reconstruction consists in letting the bulk and edge residual belong to different polynomial spaces. Notably, we assume that $r^K \in \tilde{V}_p$, whereas we let $r^e \in \Lambda_p^I$, where we have set $\Lambda_p^I := \mathbb{P}_p(\mathcal{E}_n^I)$.

Define a flux $\boldsymbol{\sigma}_{p-1}^\Delta$ in a distributional sense as follows:

$$\operatorname{div} \boldsymbol{\sigma}_{p-1}^\Delta = r \in (H_0^1(\Omega))^*. \quad (6)$$

We can interpret $\boldsymbol{\sigma}_{p-1}^\Delta$ as follows:

$$\boldsymbol{\sigma}_p^\Delta \approx \nabla \tilde{u}_p - \nabla \tilde{u} \in (H_0^1(\Omega))^*.$$

Using (4) and (6) implies that $\boldsymbol{\sigma}_{p-1}^\Delta$ satisfies

$$\begin{cases} \operatorname{div} \boldsymbol{\sigma}_{p-1}^\Delta = r^K \in \mathbb{P}_{p-1}(K) & \text{in all } K \in \mathcal{T}_n \\ \llbracket \boldsymbol{\sigma}_{p-1}^\Delta \rrbracket = r^e \in \mathbb{P}_{p-1}(e) & \text{on all } e \in \mathcal{E}_n^I. \end{cases} \quad (7)$$

The information about the homogeneous Dirichlet boundary conditions is implicitly contained in the two residuals through \tilde{u}_p . We rewrite (7) as a hybridized mixed method with flux and primal variable given by $\boldsymbol{\sigma}_p^\Delta$ and u_{p-1} , respectively. More precisely, we write

$$\begin{cases} \text{find } (\boldsymbol{\sigma}_{p-1}^\Delta, u_{p-1}, \lambda_{p-1}^I) \in \boldsymbol{\Sigma}_{p-1} \times V_{p-1} \times \Lambda_{p-1}^I \text{ such that} \\ a(\boldsymbol{\sigma}_{p-1}^\Delta, \boldsymbol{\tau}_{p-1}) + b(\boldsymbol{\tau}_{p-1}, u_{p-1}) + c(\boldsymbol{\tau}_{p-1}, \lambda_{p-1}^I) = 0 & \forall \boldsymbol{\tau}_{p-1} \in \boldsymbol{\Sigma}_{p-1} \\ b(\boldsymbol{\sigma}_{p-1}^\Delta, v_{p-1}) = (r^K, v_{p-1})_{0,\Omega} & \forall v_{p-1} \in V_{p-1} \\ c(\boldsymbol{\sigma}_{p-1}^\Delta, \mu_{p-1}^I) = (r^e, \mu_{p-1}^I)_{0,\mathcal{E}_n^I} & \forall \mu_{p-1}^I \in \Lambda_{p-1}^I, \end{cases} \quad (8)$$

where we picked the spaces

$$\begin{aligned} \boldsymbol{\Sigma}_{p-1} &:= \{ \boldsymbol{\tau}_{p-1} \in [L^2(\Omega)]^2 \mid \boldsymbol{\tau}_{p-1}|_K \in \mathbb{RT}_{p-1}(K) \forall K \in \mathcal{T}_n \}, \\ V_{p-1} &:= \mathbb{P}_{p-1}(\mathcal{T}_n), \\ \Lambda_{p-1} &:= \mathbb{P}_{p-1}(\mathcal{E}_n^I), \end{aligned} \quad (9)$$

being $\mathbb{RT}_p(K)$ the local Raviart-Thomas space of order $p \in \mathbb{N}_0$ on element K , and the bilinear forms

$$\begin{aligned} a(\boldsymbol{\sigma}_{p-1}, \boldsymbol{\tau}_{p-1}) &:= (\boldsymbol{\sigma}_{p-1}, \boldsymbol{\tau}_{p-1})_{0,\Omega}, \\ b(\boldsymbol{\tau}_{p-1}, u_{p-1}) &:= -(\operatorname{div} \boldsymbol{\tau}_{p-1}, u_{p-1})_{0,\Omega}, \\ c(\boldsymbol{\tau}_{p-1}, \mu_{p-1}^I) &:= (\llbracket \boldsymbol{\tau}_{p-1} \rrbracket, \mu_{p-1}^I)_{0,\mathcal{E}_n^I}. \end{aligned} \quad (10)$$

In the literature, the space $\boldsymbol{\Sigma}_{p-1}$ is known as the broken, hybridized Raviart-Thomas space of order $p-1$. No degrees of freedom coupling takes place at the interface between two elements. Rather, the communication between local Raviart-Thomas spaces takes place in a mortar fashion through the Lagrange multipliers in the space Λ_{p-1} .

Next, we discuss the localized version of the above problem. With each vertex $\nu \in \mathcal{V}_n$, we associate the partition of unity function $\tilde{\varphi}_\nu \in \tilde{V}_p$, i.e., the standard hat function with value 1 at ν and 0 at all other vertices, and localize the bulk and edge residuals in (5) as follows: for all $\nu \in \mathcal{V}_n$,

$$r_\nu^K := \tilde{\varphi}_\nu(f + \Delta \tilde{u}_p) \in \mathbb{P}_p(K) \quad \forall K \in \mathcal{T}_n, \quad r_\nu^e := \tilde{\varphi}_\nu \llbracket \nabla \tilde{u}_p \rrbracket \in \mathbb{P}_p(e) \quad \forall e \in \mathcal{E}_n^I. \quad (11)$$

Proceeding as above, on each vertex patch

$$\omega_\nu := \bigcup \{K \in \mathcal{T}_n \mid \nu \text{ is a vertex of } K\}, \quad (12)$$

we introduce the following local problems: if ν is an interior vertex,

$$\begin{cases} \text{find } (\boldsymbol{\sigma}_p^\nu, u_p^\nu, \lambda_p^{\nu,I}) \in \boldsymbol{\Sigma}_p^0(\omega_\nu) \times V_p^*(\omega_\nu) \times \Lambda_p^I(\omega_\nu) \text{ such that} \\ a^{\omega_\nu}(\boldsymbol{\sigma}_p^\nu, \boldsymbol{\tau}_p^\nu) + b^{\omega_\nu}(\boldsymbol{\tau}_p^\nu, u_p^\nu) + c^{\omega_\nu}(\boldsymbol{\tau}_p^\nu, \lambda_p^{\nu,I}) = 0 & \forall \boldsymbol{\tau}_p^\nu \in \boldsymbol{\Sigma}_p^0(\omega_\nu) \\ b^{\omega_\nu}(\boldsymbol{\sigma}_p^\nu, v_p^\nu) = (r_\nu^K, v_p^\nu)_{0, \omega_\nu} & \forall v_p^\nu \in V_p^*(\omega_\nu) \\ c^{\omega_\nu}(\boldsymbol{\sigma}_p^\nu, \mu_p^{\nu,I}) = (r_\nu^e, \mu_p^{\nu,I})_{0, \mathcal{E}_n^I(\omega_\nu)} & \forall \mu_p^{\nu,I} \in \Lambda_p^I(\mathcal{E}_n^I(\omega_\nu)), \end{cases}$$

whereas, if ν is a boundary vertex,

$$\begin{cases} \text{find } (\boldsymbol{\sigma}_p^\nu, u_p^\nu, \lambda_p^{\nu,I}) \in \boldsymbol{\Sigma}_p^{0, \partial\Omega}(\omega_\nu) \times V_p(\omega_\nu) \times \Lambda_p^I(\omega_\nu) \text{ such that} \\ a^{\omega_\nu}(\boldsymbol{\sigma}_p^\nu, \boldsymbol{\tau}_p^\nu) + b^{\omega_\nu}(\boldsymbol{\tau}_p^\nu, u_p^\nu) + c^{\omega_\nu}(\boldsymbol{\tau}_p^\nu, \lambda_p^{\nu,I}) = 0 & \forall \boldsymbol{\tau}_p^\nu \in \boldsymbol{\Sigma}_p^{0, \partial\Omega}(\omega_\nu) \\ b^{\omega_\nu}(\boldsymbol{\sigma}_p^\nu, v_p) = (r_\nu^K, v_p)_{0, \omega_\nu} & \forall v_p \in V_p(\omega_\nu) \\ c^{\omega_\nu}(\boldsymbol{\sigma}_p^\nu, \mu_p^{\nu,I}) = (r_\nu^e, \mu_p^{\nu,I})_{0, \mathcal{E}_n^I(\omega_\nu)} & \forall \mu_p^{\nu,I} \in \Lambda_p^I(\mathcal{E}_n^I(\omega_\nu)), \end{cases}$$

where the involved spaces and bilinear forms are the obvious counterparts of those in (9) and (10), and

$$\begin{aligned} \boldsymbol{\Sigma}_p^0(\omega_\nu) &:= \{ \boldsymbol{\tau}_p \in \boldsymbol{\Sigma}_p(\omega_\nu) \mid \mathbf{n}_e \cdot \boldsymbol{\tau}_p|_e = 0 \quad \forall e \subset \partial\omega_\nu \}, \\ \boldsymbol{\Sigma}_p^{0, \partial\Omega}(\omega_\nu) &:= \{ \boldsymbol{\tau}_p \in \boldsymbol{\Sigma}_p(\omega_\nu) \mid \mathbf{n}_e \cdot \boldsymbol{\tau}_p|_e = 0 \quad \forall e \subset \partial\omega_\nu, \nu \notin e \}, \\ V_p^*(\omega_\nu) &:= \left\{ v_p \in V_p(\omega_\nu) \mid \int_{\omega_\nu} v_p = 0 \right\}. \end{aligned}$$

In [6], it was proven that the error estimator

$$\boldsymbol{\sigma}_p := \sum_{\nu \in \mathcal{V}_n} \boldsymbol{\sigma}_p^\nu$$

is reliable and efficient with constants independent of h and p .

In Sections 3 and 4 below, we shall generalize the finite element setting to the virtual element one.

3. THE VIRTUAL ELEMENT SETTING

Here, we introduce several virtual element spaces, which we shall use in the design of the hybridized local flux reconstruction in Section 4 below. Primal virtual elements are detailed in Section 3.1, whereas we design couples of broken, mixed virtual elements in Section 3.2. We also introduce skeletal, broken polynomial spaces in Section 3.3, that will play the role of the hybridization space. As a matter of notation, we shall denote the primal, scalar variable with a tilde on top when considered as solution to the primal formulation, and without tilde when appearing in the mixed formulation.

3.1. Primal virtual elements. Here, we follow [3] and briefly recall the primal virtual element method for the Poisson problem (2).

3.1.1. *Primal virtual element spaces.* Given $p \in \mathbb{N}$, for all $K \in \mathcal{T}_n$, we introduce the primal local space

$$\tilde{V}_p(K) := \{\tilde{v}_p \in \mathcal{C}^0(\bar{K}) \mid \tilde{v}_{p|e} \in \mathbb{P}_p(e) \forall e \in \mathcal{E}_n, \Delta \tilde{v}_p \in \mathbb{P}_{p-2}(K)\}.$$

We have that $\mathbb{P}_p(K) \subseteq \tilde{V}_p(K)$. Next, consider $\{m_\alpha^K\}_{|\alpha|=0}^{p-2}$ any basis of $\mathbb{P}_{p-2}(K)$, whose elements are invariant with respect to translations and dilations. The following set of linear functionals of $\tilde{V}_p(K)$ is a set of unisolvent degrees of freedom [3]: given $\tilde{v}_p \in \tilde{V}_p(K)$,

- the point values of \tilde{v}_p at the vertices of K ;
- for each $e \in \mathcal{E}^K$, the point values of \tilde{v}_p at the p internal Gauß-Lobatto nodes of e ;
- the scaled moments

$$\frac{1}{|K|} \int_K \tilde{v}_p m_\alpha^K \quad \forall |\alpha| = 0, \dots, p-2.$$

The global virtual element space together with its set of degrees of freedom is constructed via a standard H^1 -conforming coupling of their local counterparts and strongly imposing the Dirichlet boundary conditions:

$$\tilde{V}_p := \{\tilde{v}_p \in \mathcal{C}^0(\bar{\Omega}) \cap H_0^1(\Omega) \mid \tilde{v}_{p|K} \in \tilde{V}_p(K) \forall K \in \mathcal{T}_n\}.$$

3.1.2. *Projectors.* Through the degrees of freedom detailed in Section 3.1.1, it is possible to compute two local orthogonal projectors onto polynomial space. The first one is the energy projector $\tilde{\Pi}_p^\nabla : \tilde{V}_p(K) \rightarrow \mathbb{P}_p(K)$ defined as follows: given \tilde{v}_p in $\tilde{V}_p(K)$,

$$\int_K \nabla q_p^K \cdot \nabla (\tilde{v}_p - \tilde{\Pi}_p^\nabla \tilde{v}_p) = 0 \quad \forall q_p^K \in \mathbb{P}_p(K), \quad \int_{\partial K} (\tilde{v}_p - \tilde{\Pi}_p^\nabla \tilde{v}_p) = 0.$$

The second one is the L^2 projector $\tilde{\Pi}_{p-2}^0 : \tilde{V}_p(K) \rightarrow \mathbb{P}_{p-2}(K)$ defined as follows: for all q_{p-2}^K in $\mathbb{P}_{p-2}(K)$ and \tilde{v}_p in $\tilde{V}_p(K)$,

$$\int_K q_{p-2}^K (\tilde{v}_p - \tilde{\Pi}_{p-2}^0 \tilde{v}_p) = 0.$$

3.1.3. *The primal virtual element method.* Following [3], we split the bilinear form $\tilde{a}(\cdot, \cdot)$ into local contributions:

$$\tilde{a}(u, v) = \sum_{K \in \mathcal{T}_n} \tilde{a}^K(u|_K, v|_K) := \sum_{K \in \mathcal{T}_n} (\nabla u, \nabla v)_{0,K} \quad \forall u, v \in H^1(\Omega).$$

We approximate each local bilinear form $\tilde{a}^K(\cdot, \cdot)$ with the following discrete counterpart: for all \tilde{u}_p and \tilde{v}_p in $\tilde{V}_p(K)$,

$$\tilde{a}_p^K(\tilde{u}_p, \tilde{v}_p) := \tilde{a}^K(\tilde{\Pi}_p^\nabla \tilde{u}_p, \tilde{\Pi}_p^\nabla \tilde{v}_p) + \tilde{S}^K((I - \tilde{\Pi}_p^\nabla) \tilde{u}_p, (I - \tilde{\Pi}_p^\nabla) \tilde{v}_p),$$

where the stabilizing term $\tilde{S}^K(\cdot, \cdot)$ is any bilinear form computable via the degrees of freedom and satisfying the following bounds: there exist positive stability constants $\tilde{\alpha}_*$ and $\tilde{\alpha}^*$ such that

$$\tilde{\alpha}_* |\tilde{v}_p|_{1,K}^2 \leq \tilde{S}^K(\tilde{v}_p, \tilde{v}_p) \leq \tilde{\alpha}^* |\tilde{v}_p|_{1,K}^2 \quad \forall \tilde{v}_p \in \ker(\tilde{\Pi}_p^\nabla). \quad (13)$$

Explicit choices of $\tilde{S}^K(\cdot, \cdot)$ will be discussed in Section 5 below. In the literature [5], it is possible to find explicit choices of the stabilizing term such that the stability constants $\tilde{\alpha}_*$ and $\tilde{\alpha}^*$ depend on p algebraically only.

The global discrete bilinear form for the primal formulation is given by the sum of the above local contributions:

$$\tilde{a}_p(\tilde{u}_p, \tilde{v}_p) := \sum_{K \in \mathcal{T}_n} \tilde{a}_p^K(\tilde{u}_p|_K, \tilde{v}_p|_K).$$

As for the discretization of the right-hand side, we pick

$$(f_p, \tilde{v}_p)_{0,\Omega} := \sum_{K \in \mathcal{T}_n} (f, \tilde{\Pi}_{p-2}^0 \tilde{v}_p)_{0,K}.$$

The primal virtual element method reads as follows:

$$\begin{cases} \text{find } \tilde{u}_p \in \tilde{V}_p \text{ such that} \\ \tilde{a}_p(\tilde{u}_p, \tilde{v}_p) = (f_p, \tilde{v}_p)_{0,\Omega} \quad \forall \tilde{v}_p \in \tilde{V}_p. \end{cases} \quad (14)$$

Method (14) is well posed; see [3].

3.2. Mixed virtual elements. Here, we introduce stable couples of broken, mixed virtual element spaces. As for the flux space, the local spaces are those introduced in [4], yet the global space consists of piecewise discontinuous functions as in [8] for the elasticity case. Furthermore, we design suitable bilinear forms appearing in the hybridized mixed formulations of Section 4 below.

3.2.1. Mixed virtual element spaces. Given $p \in \mathbb{N}_0$, for all $K \in \mathcal{T}_n$, we introduce the local mixed space [4]

$$\begin{aligned} \Sigma_p(K) := \{ \boldsymbol{\tau}_p \in H(\operatorname{div}, K) \cap H(\operatorname{rot}, \Omega) \mid \mathbf{n}_K \cdot \boldsymbol{\tau}_p|_e \in \mathbb{P}_p(e) \forall e \in \mathcal{E}^K, \\ \operatorname{div} \boldsymbol{\tau}_p \in \mathbb{P}_p(K), \operatorname{rot} \boldsymbol{\tau}_p \in \mathbb{P}_{p-1}(K) \}. \end{aligned}$$

We have that $[\mathbb{P}_p(K)]^2 \subseteq \Sigma_p(K)$. Next, consider the splitting of $[\mathbb{P}_p(K)]^2$ into

$$[\mathbb{P}_p(K)]^2 = \mathcal{G}_p(K) \oplus \mathcal{G}_p^\perp(K), \quad \mathcal{G}_p(K) := \nabla \mathbb{P}_{p+1}(K),$$

where $\mathcal{G}^\perp(K)$ is any completion of $\mathcal{G}_p(K)$ in $[\mathbb{P}_p(K)]^2$. Denote the dimension of $\mathcal{G}_p(K)$ and $\mathcal{G}_p^\perp(K)$ by \mathfrak{g}_p and \mathfrak{g}_p^\perp , respectively. Moreover, consider $\{\mathbf{g}_\alpha\}_{\alpha=1}^{\mathfrak{g}_p}$ and $\{\mathbf{g}_\alpha^\perp\}_{\alpha=1}^{\mathfrak{g}_p^\perp}$ any bases of $\mathcal{G}_p(K)$ and $\mathcal{G}_p^\perp(K)$, consisting of elements that are invariant with respect to translations and dilations; we refer to [?] for explicit choices of such bases. The following set of linear functionals of $\Sigma_p(K)$ is a set of unsolvent degrees of freedom [4]: given $\boldsymbol{\tau}_p \in \Sigma_p(K)$,

- for each $e \in \mathcal{E}^K$, the point values of $\boldsymbol{\tau}_p$ at the $p+1$ Gauß quadrature nodes of e ;
- the gradient-type moments up to order $p-1$

$$\frac{1}{|K|} \int_K \boldsymbol{\tau}_p \cdot \mathbf{g}_\alpha \quad \forall \alpha = 1, \dots, \mathfrak{g}_{p-1};$$

- the “completion”-type moments up to order p

$$\frac{1}{|K|} \int_K \boldsymbol{\tau}_p \cdot \mathbf{g}_\alpha^\perp \quad \forall \alpha = 1, \dots, \mathfrak{g}_p^\perp.$$

Differently from the standard Raviart-Thomas approach of [4], we do not construct the corresponding global space by imposing $H(\operatorname{div})$ conformity. Rather, we hybridize the space, see [1, 8], and therefore consider the following global discontinuous mixed space:

$$\Sigma_p := \{ \boldsymbol{\tau}_p \in [L^2(\Omega)]^2 \mid \boldsymbol{\tau}_p|_K \in \Sigma_p(K) \}.$$

Since we do not match the edge degrees of freedom, we do not impose any boundary condition in the space. Rather, the boundary conditions will be imposed in a mortar way through the hybridized variable.

We further introduce the space taking care of the scalar variable. To the aim, we simply set

$$V_p := \mathbb{P}_p(\mathcal{T}_n).$$

3.2.2. Projectors. Through the degrees of freedom detailed in Section 3.2.1, it is possible to compute [4] a vector, piecewise L^2 orthogonal projector $\Pi_p^0 : \Sigma_p(K) \rightarrow [\mathbb{P}_p(K)]^2$, which is defined as follows: for all \mathbf{q}_p^K and $\boldsymbol{\tau}_p \in \Sigma_p(K)$,

$$(\mathbf{q}_p^K, \boldsymbol{\tau}_p - \Pi_p^0 \boldsymbol{\tau}_p)_{0,K} = 0.$$

3.2.3. Mixed virtual element bilinear forms. Following [4], we split the bilinear form $a(\cdot, \cdot) := (\cdot, \cdot)_{0,\Omega}$ into local contributions:

$$a(\boldsymbol{\sigma}, \boldsymbol{\tau}) = \sum_{K \in \mathcal{T}_n} a^K(\boldsymbol{\sigma}|_K, \boldsymbol{\tau}|_K) := \sum_{K \in \mathcal{T}_n} (\boldsymbol{\sigma}, \boldsymbol{\tau})_{0,K} \quad \forall \boldsymbol{\sigma}, \boldsymbol{\tau} \in [L^2(\Omega)]^2.$$

We approximate each local bilinear form $a_p^K(\cdot, \cdot)$ with the following discrete counterpart: for all $\boldsymbol{\sigma}_p$ and $\boldsymbol{\tau}_p$ in $\Sigma_p(K)$,

$$a_p^K(\boldsymbol{\sigma}_p, \boldsymbol{\tau}_p) = a^K(\Pi_p^0 \boldsymbol{\sigma}_p, \Pi_p^0 \boldsymbol{\tau}_p) + S^K((\mathbf{I} - \Pi_p^0) \boldsymbol{\sigma}_p, (\mathbf{I} - \Pi_p^0) \boldsymbol{\tau}_p), \quad (15)$$

where the stabilizing term $S^K(\cdot, \cdot)$ is any bilinear form computable via the degrees of freedom and satisfying the following bounds: there exist positive stability constants α_* and α^* such that

$$\alpha_* \|\boldsymbol{\tau}_p\|_{0,K}^2 \leq S^K(\boldsymbol{\tau}_p, \boldsymbol{\tau}_p) \leq \alpha^* \|\boldsymbol{\tau}_p\|_{0,K}^2 \quad \forall \boldsymbol{\tau}_p \in \ker(\Pi_p^0). \quad (16)$$

An explicit choice of $S^K(\cdot, \cdot)$ will be derived and analyzed in Appendix A below. Importantly, we shall show that the stability constants depend on p algebraically only.

The global discrete bilinear form for mixed virtual elements is given by the sum of the above local contributions:

$$a_p(\boldsymbol{\sigma}_p, \boldsymbol{\tau}_p) := \sum_{K \in \mathcal{T}_n} a_p^K(\boldsymbol{\sigma}_p|_K, \boldsymbol{\tau}_p|_K).$$

The choice of the degrees of freedom in Section 3.2.1 allows for the explicit computation of the local divergence of any function $\boldsymbol{\tau}_p \in \boldsymbol{\Sigma}_p(K)$ on each element $K \in \mathcal{T}_n$; see [4]. Therefore, we also define the exactly computable bilinear form

$$b(\boldsymbol{\tau}_p, v_p) := \sum_{K \in \mathcal{T}_n} (\operatorname{div} \boldsymbol{\tau}_p, v_p)_{0,K} \quad \forall \boldsymbol{\tau}_p \in \boldsymbol{\Sigma}_p, \forall v_p \in V_p.$$

3.3. Hybridized virtual elements. Here, we introduce piecewise discontinuous polynomial spaces, and the related bilinear forms and their properties, which will be instrumental in the design of the hybridized flux reconstruction of Section 4 below.

3.3.1. Hybrid virtual element spaces. Given $p \in \mathcal{T}_n$, we introduce the hybridization space

$$\Lambda_p^I := \mathbb{P}_p(\mathcal{E}_n^I).$$

The following set of linear functionals is a global set of degrees of freedom for Λ_p^I : given $\lambda_p^I \in \Lambda_p^I$,

- for each $e \in \mathcal{E}_n^I$, the point values of λ_p^I at the $p+1$ Gauß nodes of e .

3.3.2. Hybrid virtual element bilinear forms. We introduce a bilinear form that will be instrumental in the design of the hybridized virtual element method. To the aim, we first define the jump operator across an internal edge $e \in \mathcal{E}_n^I$: for any $\boldsymbol{\tau} \in H(\operatorname{div}, \mathcal{T}_n)$,

$$[\![\boldsymbol{\tau}]\!]_e := [\![\boldsymbol{\tau}]\!] = \boldsymbol{\tau}|_{K^+} \cdot \mathbf{n}_{K^+} + \boldsymbol{\tau}|_{K^-} \cdot \mathbf{n}_{K^-} \quad \forall e \in \mathcal{E}_n^I, e \in \mathcal{E}^{K^+} \cap \mathcal{E}^{K^-}.$$

We define the bilinear form $c(\cdot, \cdot) : \boldsymbol{\Sigma}_p \times \Lambda_p^I \rightarrow \mathbb{R}$ as

$$c(\boldsymbol{\tau}_p, \mu_p^I) := \sum_{e \in \mathcal{E}_n^I} ([\![\boldsymbol{\tau}_p]\!]_e, \mu_p^I)_{0,e} \quad \forall \boldsymbol{\tau}_p \in \boldsymbol{\Sigma}_p, \forall \mu_p^I \in \Lambda_p^I.$$

Introduce the weighted, broken divergence norm:

$$\|\boldsymbol{\tau}\|_{\operatorname{div}, \mathcal{T}_n}^2 = \sum_{K \in \mathcal{T}_n} (h_K^{-1} \|\boldsymbol{\tau}\|_{0,K}^2 + h_K \|\operatorname{div} \boldsymbol{\tau}\|_{0,K}^2) \quad \forall \boldsymbol{\tau} \in H(\operatorname{div}, \mathcal{T}_n).$$

To analyze hybridized virtual elements, it is convenient to prove the existence of a stable, broken $H(\operatorname{div})$ lifting operator $\mathcal{L} : L^2(\mathcal{E}_n^I) \rightarrow H(\operatorname{div}, \mathcal{T}_n)$ such that

$$\|\mathcal{L}(\mu_p^I)\|_{\operatorname{div}, \mathcal{T}_n} \leq \beta_c \|\mu_p^I\|_{0, \mathcal{E}_n^I}, \quad [\![\mathcal{L}(\mu_p^I)]\!]_e = \mu_p^I \quad \forall e \in \mathcal{E}_n^I, \quad (17)$$

where β_c is a positive constant, independent of the discretization parameters.

Proposition 3.1. *There exists a stable lifting operator \mathcal{L} as in (17).*

Proof. For all $\mu_p^I \in \Lambda_p^I$, we have to construct a flux $\mathcal{L}(\mu_p^I) = \boldsymbol{\tau}_p \in \boldsymbol{\Sigma}_p$ satisfying (17). To the aim, we define $\boldsymbol{\tau}_p$ in each element K as $\boldsymbol{\tau}_p = \nabla \varphi$, where φ is the solution to the following local elliptic problems on each $K \in \mathcal{T}_n$:

$$\begin{cases} \Delta \varphi = c_K & \text{in } K \\ \mathbf{n}_K \cdot \nabla \varphi = \frac{1}{2} \mu_p^I & \text{on each } e \in \mathcal{E}^K \cap \mathcal{E}_n^I \\ \mathbf{n}_K \cdot \nabla \varphi = 0 & \text{on each } e \in \mathcal{E}^K \cap \mathcal{E}_n^D \\ \int_K \varphi = 0, \end{cases}$$

where $c_K \in \mathbb{R}$ is fixed so that the following compatibility condition is valid:

$$c_K = \frac{1}{2} |K|^{-1} \sum_{e \in \mathcal{E}^K \cap \mathcal{E}_n^I} (\mu_p^I, 1)_{0,e}. \quad (18)$$

The above Neumann problem is well posed since the compatibility condition (18) is valid.

The flux $\boldsymbol{\tau}_p = \nabla\varphi$ satisfies the following properties:

$$\begin{aligned} \operatorname{div} \boldsymbol{\tau}_p|_K &= c_K, & \|\boldsymbol{\tau}_p\|_{0,K} &= |\varphi|_{1,K}, & \|\operatorname{div} \boldsymbol{\tau}_p\|_{0,K} &= |K|^{\frac{1}{2}}|c_K| & \forall K \in \mathcal{T}_n, \\ \llbracket \boldsymbol{\tau}_p \rrbracket_e &= \mu_p^I|_e & \forall e \in \mathcal{E}_n^I. \end{aligned} \quad (19)$$

Additionally, for all $K \in \mathcal{T}_n$, we observe that

$$\|\boldsymbol{\tau}_p\|_{0,K}^2 = \int_K \nabla\varphi \cdot \nabla\varphi = - \int_K (\Delta\varphi)\varphi + \int_{\partial K} (\mathbf{n}_K \cdot \nabla\varphi)\varphi.$$

The first term on the right-hand side is zero, since $\Delta\varphi$ is constant and φ has zero average over K . Thus, the trace and the Poincaré inequalities yield

$$\|\boldsymbol{\tau}_p\|_{0,K}^2 \leq \|\mathbf{n}_K \cdot \nabla\varphi\|_{0,\partial K \setminus \partial\Omega} \|\varphi\|_{0,\partial K} \lesssim \|\mu_p^I\|_{0,\partial K \setminus \partial\Omega} h_K^{\frac{1}{2}} |\varphi|_{1,K} \stackrel{(19)}{=} \|\mu_p^I\|_{0,\partial K \setminus \partial\Omega} h_K^{\frac{1}{2}} \|\boldsymbol{\tau}_p\|_{0,K}.$$

Furthermore, we have

$$\|\operatorname{div} \boldsymbol{\tau}_p\|_{0,K} \stackrel{(18)}{=} |K|^{\frac{1}{2}}|c_K| \stackrel{(19)}{\lesssim} |K|^{-\frac{1}{2}} \|\mu_p^I\|_{0,\partial K \setminus \partial\Omega} |e|^{\frac{1}{2}} \lesssim h_K^{-\frac{1}{2}} \|\mu_p^I\|_{0,\partial K \setminus \partial\Omega}.$$

Collecting the last two bounds and summing over all the elements yield the assertion. \square

4. THE HYBRIDIZED VIRTUAL ELEMENT HYPERCIRCLE AND LOCAL FLUX RECONSTRUCTION

Here, we introduce the global and local flux reconstruction in hybridized virtual elements. The two formulations allow us to propose computable error estimators that are reliable and efficient. The global and local versions are detailed in Sections 4.1 and 4.2, respectively.

4.1. The hybridized global flux reconstruction with the virtual element method. Here, we introduce a hybridized mixed VEM mimicking its finite element counterpart (8).

Set

$$r^K := f + \Delta \tilde{\Pi}_p^\nabla \tilde{u}_p \in \mathbb{P}_{p-1}(K) \quad \forall K \in \mathcal{T}_n, \quad r^e := \llbracket \nabla \tilde{\Pi}_p^\nabla \tilde{u}_p \rrbracket \in \mathbb{P}_{p-1}(e) \quad \forall e \in \mathcal{E}_n^I, \quad (20)$$

where \tilde{u}_p solves the primal VEM (14).

We consider the method

$$\begin{cases} \text{find } (\boldsymbol{\sigma}_{p-1}^\Delta, u_{p-1}, \lambda_{p-1}^I) \in \boldsymbol{\Sigma}_{p-1} \times V_{p-1} \times \Lambda_{p-1}^I \text{ such that} \\ a_{p-1}(\boldsymbol{\sigma}_{p-1}^\Delta, \boldsymbol{\tau}_{p-1}) + b(\boldsymbol{\tau}_{p-1}, u_{p-1}) + c(\boldsymbol{\tau}_{p-1}, \lambda_{p-1}^I) = 0 & \forall \boldsymbol{\tau}_{p-1} \in \boldsymbol{\Sigma}_{p-1} \\ b(\boldsymbol{\sigma}_{p-1}^\Delta, v_{p-1}) = (r^K, v_{p-1})_{0,\Omega} & \forall v_{p-1} \in V_{p-1} \\ c(\boldsymbol{\sigma}_{p-1}^\Delta, \mu_{p-1}^I) = (r^e, \mu_{p-1}^I)_{0,\mathcal{E}_n^I} & \forall \mu_{p-1}^I \in \Lambda_{p-1}^I, \end{cases} \quad (21)$$

where the discrete spaces and bilinear form are those introduced in Section 3.

Problem (21) is well posed. To see this, we observe that Proposition 3.1 guarantees the existence of a stable lifting operator, which allows us to rewrite problem (21) with zero right-hand side in the third equation.

This implies that the flux and primal solutions are in fact solutions to a standard mixed problem, which is well posed. The bilinear form $a_p(\cdot, \cdot)$ is coercive on $\boldsymbol{\Sigma}_p$. Moreover, the bilinear form $b(\cdot, \cdot)$ satisfies the following discrete inf-sup condition:

$$\inf_{v_p \in V_p} \sup_{\boldsymbol{\tau}_p \in \boldsymbol{\Sigma}_p \cap H(\operatorname{div}, \Omega)} \frac{b(\boldsymbol{\tau}_p, v_p)}{(\sum_{K \in \mathcal{T}_n} \|\boldsymbol{\tau}_p\|_{\operatorname{div}, K}^2)^{\frac{1}{2}} \|v_p\|_{0,\Omega}} \geq \beta_b \quad \forall p \in \mathbb{N}_0, \quad (22)$$

where β_b is a positive constant independent of h and p . The p -independence of β_b is proven in [7, Theorem 2.8].

Therefore, there exist unique $\boldsymbol{\sigma}_{p-1}^\Delta$ and u_{p-1} solutions to (21), with continuous dependence on the data. The existence, uniqueness, and continuous dependence on the data of the hybridized solution λ_{p-1}^I are a consequence of the first line of the method, picking a test function $\boldsymbol{\tau}_{p-1}$ such that

$$c(\boldsymbol{\tau}_{p-1}, \lambda_{p-1}^I) = c(\lambda_{p-1}^I, \lambda_{p-1}^I)$$

the L^2 skeleton coercivity of the bilinear form $c(\cdot, \cdot)$, and the stability property of the lifting operator \mathcal{L} in (17).

Eventually, we introduce a global error estimator based on the global flux reconstruction:

$$\eta^2 := \|\boldsymbol{\sigma}_{p-1}^\Delta\|_{a_{p-1}}^2 + \sum_{K \in \mathcal{T}_n} \tilde{S}^K((I - \tilde{\Pi}_p^\nabla)\tilde{u}_p, (I - \tilde{\Pi}_p^\nabla)\tilde{u}_p), \quad (23)$$

which we shall analyze in Section 4.2 below.

4.2. The hybridized global flux reconstruction: reliability and efficiency. Here, we prove the reliability and efficiency of the error estimator η defined in (23). We begin by proving its reliability.

Theorem 4.1. *The error estimator η defined in (23) is reliable, i.e., given \tilde{u} and \tilde{u}_p the primal solutions to (2) and (14), and $\boldsymbol{\sigma}_{p-1}^\Delta$ the solution to (21), the following bound is valid:*

$$|\tilde{u} - \tilde{u}_p|_{1,K}^2 \leq (1 + \alpha_*^{-1}) \|\boldsymbol{\sigma}_{p-1}^\Delta\|_{a_{p-1}}^2 + \tilde{\alpha}_*^{-1} \sum_{K \in \mathcal{T}_n} \tilde{S}^K((I - \tilde{\Pi}_p^\nabla)\tilde{u}_p, (I - \tilde{\Pi}_p^\nabla)\tilde{u}_p),$$

where $\tilde{\alpha}_*$ and α_* are stability constants appearing in (13) and (16).

Proof. For all $\tilde{v} \in \tilde{V}$, we have

$$\begin{aligned} (\nabla(\tilde{u} - \tilde{u}_p), \nabla\tilde{v})_{0,\Omega} &= -(\Delta\tilde{u}, \tilde{v})_{0,\Omega} - (\nabla\tilde{u}_p, \nabla\tilde{v})_{0,\Omega} \\ &= \sum_{K \in \mathcal{T}_n} [(f + \Delta\tilde{\Pi}_p^\nabla\tilde{u}_p, \tilde{v})_{0,K} - (\Delta\tilde{\Pi}_p^\nabla\tilde{u}_p, \tilde{v})_{0,K}] - (\nabla\tilde{u}_p, \nabla\tilde{v})_{0,\Omega} \\ &= \sum_{K \in \mathcal{T}_n} (r^K, \tilde{v})_{0,K} - \sum_{e \in \mathcal{E}_n^I} (r^e, \tilde{v})_{0,e} + \sum_{K \in \mathcal{T}_n} (\nabla(\tilde{\Pi}_p^\nabla\tilde{u}_p - \tilde{u}_p), \nabla\tilde{v})_{0,K}. \end{aligned}$$

From the definition of the virtual element spaces and the global hybridized problem (21), we have that

$$\operatorname{div} \boldsymbol{\sigma}_{p-1}^\Delta|_K = r^K \quad \forall K \in \mathcal{T}_n, \quad \llbracket \boldsymbol{\sigma}_{p-1}^\Delta \rrbracket_e = r^e \quad \forall e \in \mathcal{E}_n^I.$$

Therefore, we can write

$$(\nabla(\tilde{u} - \tilde{u}_p), \nabla\tilde{v})_{0,\Omega} = \sum_{K \in \mathcal{T}_n} \left[-(\boldsymbol{\sigma}_{p-1}^\Delta, \nabla\tilde{v})_{0,K} + (\nabla(\tilde{\Pi}_p^\nabla\tilde{u}_p - \tilde{u}_p), \nabla\tilde{v})_{0,K} \right].$$

We focus on the local contributions of the second term on the right-hand side:

$$\begin{aligned} (\nabla(\tilde{\Pi}_p^\nabla\tilde{u}_p - \tilde{u}_p), \nabla\tilde{v})_{0,K} &\leq |\tilde{\Pi}_p^\nabla\tilde{u}_p - \tilde{u}_p|_{1,K} |\tilde{v}|_{1,K} \\ &\stackrel{(16)}{\leq} \tilde{\alpha}_*^{-1} \tilde{S}^K((I - \tilde{\Pi}_p^\nabla)\tilde{u}_p, (I - \tilde{\Pi}_p^\nabla)\tilde{u}_p)^{\frac{1}{2}} |\tilde{v}|_{1,K}. \end{aligned}$$

Summing over all the elements and collecting the above bounds yield the assertion picking $\tilde{v} = \tilde{u} - \tilde{u}_p$. \square

Next, we investigate the efficiency of the error estimator η defined in (23), which is proven up to the presence of a higher order converging term.

Theorem 4.2. *The error estimator η defined in (23) is efficient, i.e., given \tilde{u} and \tilde{u}_p the primal solutions to (2) and (14), and $\boldsymbol{\sigma}_{p-1}^\Delta$ the solution to (21), the following bound is valid:*

$$\|\boldsymbol{\sigma}_{p-1}^\Delta\|_{a_{p-1}}^2 \leq (1 + \alpha^*) \left[|\tilde{u} - \tilde{u}_p|_{1,\mathcal{T}_n}^2 + |\tilde{u} - \tilde{\Pi}_p^\nabla\tilde{u}|_{1,\mathcal{T}_n}^2 \right], \quad (24)$$

where α^* is a stability constant appearing in (16).

Proof. Define the discrete kernel

$$\begin{aligned} \mathbf{Z}_{p-1} &:= \{ \boldsymbol{\tau}_{p-1} \in \boldsymbol{\Sigma}_{p-1} \mid b(\boldsymbol{\tau}_{p-1}, v_{p-1}) = (r^K, v_{p-1})_{0,\Omega} \quad \forall v_{p-1} \in V_{p-1}, \\ &\quad c(\boldsymbol{\tau}_{p-1}, \mu_{p-1}^I) = (r^e, \mu_{p-1}^I)_{0,\mathcal{E}_n^I} \quad \forall \mu_{p-1}^I \in \Lambda_{p-1}^I \} \end{aligned} \quad (25)$$

and

$$\begin{aligned} \mathbf{Z} &:= \{ \boldsymbol{\tau} \in H(\operatorname{div}, \mathcal{T}_n) \cap H(\operatorname{rot}, \mathcal{T}_n) \mid \operatorname{div} \boldsymbol{\tau}|_K = r^K \quad \forall K \in \mathcal{E}^K, \\ &\quad c(\boldsymbol{\tau}, \mu_{p-1}^I) = (r^e, \mu_{p-1}^I)_{0,\mathcal{E}_n^I} \quad \forall \mu_{p-1}^I \in \Lambda_{p-1}^I \}. \end{aligned}$$

A consequence of standard saddle point problem theory is that the solution σ_{p-1}^Δ to (21) satisfies

$$\|\sigma_{p-1}^\Delta\|_{a_{p-1}} = \inf_{\tau_{p-1} \in \mathbf{Z}_{p-1}} \|\tau_{p-1}\|_{a_{p-1}} \leq \|\tau_{p-1}^\Delta\|_{a_{p-1}} \quad \forall \tau_{p-1}^\Delta \in \mathbf{Z}_{p-1}.$$

Therefore, it suffices to show that there exists $\tau_{p-1}^\Delta \in \mathbf{Z}_{p-1}$ satisfying (24). We define τ_{p-1}^Δ as the interpolant of a function $\tau^\Delta \in \mathbf{Z}$ in \mathbf{Z}_{p-1} that we now design.

On each $K \in \mathcal{T}_n$, we set $\tau^\Delta = \nabla w$, where w solves

$$\begin{cases} \Delta w = r^K (= f + \Delta \tilde{\Pi}_p^\nabla \tilde{u}_p) & \text{in } K \\ \mathbf{n}_K \cdot \nabla w = \mathbf{n}_K \cdot (\nabla \tilde{\Pi}_p^\nabla \tilde{u}_p - \nabla \tilde{u}) & \forall e \in \mathcal{E}^K \\ \int_K w = 0. \end{cases}$$

The above local problems are well posed: the compatibility condition between the right-hand side and the Neumann data follows from an integration by parts. It is immediate to check that $\tau^\Delta \in \mathbf{Z}$: \tilde{u} has continuous Neumann traces across internal edges.

Recalling that the discrete bilinear form $a_{p-1}(\cdot, \cdot)$ is computed only through the degrees of freedom of functions in mixed virtual element spaces, we also have

$$\|\tau_{p-1}^\Delta\|_{a_{p-1}} = \|\tau^\Delta\|_{a_{p-1}}.$$

This, Remark 1 below, the fact that $\operatorname{div} \tau^\Delta|_K$ belongs to $\mathbb{P}_{p-1}(K)$ for all $K \in \mathcal{T}_n$, and (16), imply

$$\|\tau_{p-1}^\Delta\|_{a_{p-1}}^2 = \|\tau^\Delta\|_{a_{p-1}}^2 \leq (1 + \alpha^*) \|\tau^\Delta\|_{0,\Omega}^2.$$

Furthermore, for all $K \in \mathcal{T}_n$, we have

$$\begin{aligned} \|\tau^\Delta\|_{0,K}^2 &= (\tau^\Delta, \nabla w)_{0,K} = -(\operatorname{div} \tau^\Delta, w)_{0,K} + (\mathbf{n}_K \cdot \tau^\Delta, w)_{0,\partial K} \\ &= -(f + \Delta \tilde{\Pi}_p^\nabla \tilde{u}_p, w)_{0,K} + (\mathbf{n}_K \cdot (\nabla \tilde{\Pi}_p^\nabla \tilde{u}_p - \nabla \tilde{u}), w)_{0,\partial K} \\ &= (\nabla (\tilde{\Pi}_p^\nabla \tilde{u}_p - \tilde{u}), \nabla w)_{0,K} \leq |\tilde{\Pi}_p^\nabla \tilde{u}_p - \tilde{u}|_{1,K} \|\tau^\Delta\|_{0,K}. \end{aligned}$$

After collecting the above estimates and summing over all the elements, we can write

$$\|\sigma_{p-1}^\Delta\|_{a_{p-1}}^2 \leq (1 + \alpha^*) |\tilde{u} - \tilde{\Pi}_p^\nabla \tilde{u}_p|_{1,\mathcal{T}_n}^2 \leq (1 + \alpha^*) (|\tilde{u} - \tilde{u}_p|_{1,\mathcal{T}_n}^2 + |\tilde{u} - \tilde{\Pi}_p^\nabla \tilde{u}_p|_{1,\mathcal{T}_n}^2).$$

The assertion follows upon using (16). \square

4.3. The hybridized localized virtual element flux reconstruction. Here, we introduce an error estimator based on local hybridized flux reconstruction.

To this aim, with each vertex $\nu \in \mathcal{V}_n$, we associate the partition of unity function $\tilde{\varphi}_\nu \in \tilde{V}_1$. Each $\tilde{\varphi}_\nu$ belongs to the lowest order primal virtual element space \tilde{V}_1 . Notably, we require that $\tilde{\varphi}_\nu$ is harmonic in each element, piecewise linear on the skeleton, and equal to 1 at vertex ν and 0 at all the others.

We localize the bulk and edge residuals in (5) as follows: for all $\nu \in \mathcal{V}_n$,

$$\begin{aligned} r_\nu^K &:= \tilde{\Pi}_1^\nabla \tilde{\varphi}_\nu (f + \Delta \tilde{\Pi}_p^\nabla \tilde{u}_p) \in \mathbb{P}_p(K) \quad \forall K \in \mathcal{T}_n(\omega_\nu), \\ r_\nu^e &:= \tilde{\varphi}_\nu [\nabla \tilde{\Pi}_p^\nabla \tilde{u}_p] \in \mathbb{P}_p(e) \quad \forall e \in \mathcal{E}_n^I(\omega_\nu). \end{aligned} \tag{26}$$

Proceeding as above, on each vertex patch ω_ν defined in (12), we introduce the following local problems: if ν is an interior vertex,

$$\begin{cases} \text{find } (\sigma_p^\nu, u_p^\nu, \lambda_p^{\nu,I}) \in \Sigma_p^0(\omega_\nu) \times V_p^*(\omega_\nu) \times \Lambda_p^I(\omega_\nu) \text{ such that} \\ a^{\omega_\nu}(\sigma_p^\nu, \tau_p^\nu) + b^{\omega_\nu}(\tau_p^\nu, u_p^\nu) + c^{\omega_\nu}(\tau_p^\nu, \lambda_p^{\nu,I}) = 0 & \forall \tau_p^\nu \in \Sigma_p^0(\omega_\nu) \\ b^{\omega_\nu}(\sigma_p^\nu, v_p^\nu) = (r_\nu^K, v_p^\nu)_{0,\omega_\nu} & \forall v_p^\nu \in V_p^*(\omega_\nu) \\ c^{\omega_\nu}(\sigma_p^\nu, \mu_p^{\nu,I}) = (r_\nu^e, \mu_p^{\nu,I})_{0,\mathcal{E}_n^I(\omega_\nu)} & \forall \mu_p^{\nu,I} \in \Lambda_p^I(\omega_\nu), \end{cases} \tag{27}$$

whereas, if ν is a boundary vertex,

$$\left\{ \begin{array}{ll} \text{find } (\boldsymbol{\sigma}_p^\nu, u_p^\nu, \lambda_p^{\nu,I}) \in \boldsymbol{\Sigma}_p^{0,\partial\Omega}(\omega_\nu) \times V_p(\omega_\nu) \times \Lambda_p^I(\omega_\nu) \text{ such that} & \\ a^{\omega_\nu}(\boldsymbol{\sigma}_p^\nu, \boldsymbol{\tau}_p^\nu) + b^{\omega_\nu}(\boldsymbol{\tau}_p^\nu, u_p^\nu) + c^{\omega_\nu}(\boldsymbol{\tau}_p^\nu, \lambda_p^{\nu,I}) = 0 & \forall \boldsymbol{\tau}_p^\nu \in \boldsymbol{\Sigma}_p^{0,\partial\Omega}(\omega_\nu) \\ b^{\omega_\nu}(\boldsymbol{\sigma}_p^\nu, v_p) = (r_\nu^K, v_p^\nu)_{0,\omega_\nu} & \forall v_p^\nu \in V_p(\omega_\nu) \\ c^{\omega_\nu}(\boldsymbol{\sigma}_p^\nu, \mu_p^{\nu,I}) = (r_\nu^e, \mu_p^{\nu,I})_{0,\mathcal{E}_n^I(\omega_\nu)} & \forall \mu_p^{\nu,I} \in \Lambda_p^I(\omega_\nu), \end{array} \right. \quad (28)$$

where the involved spaces and bilinear forms are the obvious counterparts of those in (9) and (10), and where

$$\begin{aligned} \boldsymbol{\Sigma}_p^0(\omega_\nu) &:= \{ \boldsymbol{\tau}_p \in \boldsymbol{\Sigma}_p(\omega_\nu) \mid \mathbf{n}_e \cdot \boldsymbol{\tau}_p|_e = 0 \quad \forall e \subset \partial\omega_\nu \}, \\ \boldsymbol{\Sigma}_p^{0,\partial\Omega}(\omega_\nu) &:= \{ \boldsymbol{\tau}_p \in \boldsymbol{\Sigma}_p(\omega_\nu) \mid \mathbf{n}_e \cdot \boldsymbol{\tau}_p|_e = 0 \quad \forall e \subset \partial\omega_\nu, \nu \notin e \}, \\ V_p^*(\omega_\nu) &:= \left\{ v_p \in V_p(\omega_\nu) \mid \int_{\omega_\nu} v_p = 0 \right\}. \end{aligned}$$

The well posedness of the above local problems follows as for the global problem (21).

We introduce the following error estimator:

$$\eta_{\text{loc}}^2 := \sum_{K \in \mathcal{T}_n} \|\boldsymbol{\sigma}_p^\Delta\|_{a_p^K}^2 + \sum_{K \in \mathcal{T}_n} \tilde{S}^K((I - \tilde{\Pi}_p^\nabla)\tilde{u}_p, (I - \tilde{\Pi}_p^\nabla)\tilde{u}_p), \quad (29)$$

where

$$\boldsymbol{\sigma}_p^\Delta := \sum_{\nu \in \mathcal{V}_n} \boldsymbol{\sigma}_p^\nu. \quad (30)$$

4.4. The hybridized localized virtual element flux reconstruction: reliability and efficiency. Here, we prove the reliability and efficiency of the error estimator η_{loc} in (29). We begin by proving the reliability.

Theorem 4.3. *The error estimator η_{loc} in (29) is reliable, i.e., given \tilde{u} and \tilde{u}_p the primal solutions to (2) and (14), and $\boldsymbol{\sigma}_p^\Delta$ as in (30) the following bound is valid:*

$$|\tilde{u} - \tilde{u}_p|_{1,\Omega}^2 \leq (1 + \alpha_*^{-1}) \|\boldsymbol{\sigma}_p^\Delta\|_{a_p}^2 + \tilde{\alpha}_*^{-1} \sum_{K \in \mathcal{T}_n} \tilde{S}^K((I - \tilde{\Pi}_p^\nabla)\tilde{u}_p, (I - \tilde{\Pi}_p^\nabla)\tilde{u}_p),$$

where $\tilde{\alpha}_*$ and α_* are stability constants appearing in (13) and (16).

Proof. Proceeding as in the proof of Theorem 4.1, we further use the property of the partition of unity functions, i.e.

$$\sum_{\nu \in \mathcal{V}^K} \tilde{\Pi}_1^\nabla \tilde{\varphi}_\nu = 1.$$

For all $\tilde{v} \in \tilde{V}$, we write

$$\begin{aligned} (\nabla(\tilde{u} - \tilde{u}_p), \nabla\tilde{v})_{0,\Omega} &= \sum_{K \in \mathcal{T}_n} [(f + \Delta\tilde{\Pi}_p^\nabla\tilde{u}_p, \tilde{v})_{0,K} - (\Delta\tilde{\Pi}_p^\nabla\tilde{u}_p, \tilde{v})_{0,K}] - (\nabla\tilde{u}_p, \nabla\tilde{v})_{0,\Omega} \\ &= \sum_{\nu \in \mathcal{V}_n} \left[\sum_{K \in \mathcal{T}_n} (r_\nu^K, \tilde{v})_{0,K} - \sum_{e \in \mathcal{E}_n^I} (r_\nu^e, \tilde{v})_{0,e} \right] + \sum_K (\nabla(\tilde{\Pi}_p^\nabla\tilde{u}_p - \tilde{u}_p), \nabla\tilde{v})_{0,\Omega}. \end{aligned}$$

Recalling the local problems (27) and (28), and using again the properties of the partition of unity, we arrive at

$$\begin{aligned} (\nabla(\tilde{u} - \tilde{u}_p), \nabla\tilde{v})_{0,\Omega} &= \sum_{K \in \mathcal{T}_n} \sum_{\nu \in \mathcal{V}^K} (\boldsymbol{\sigma}_p^\nu, \nabla\tilde{v})_{0,K} + \sum_{K \in \mathcal{T}_n} (\nabla(\tilde{\Pi}_p^\nabla\tilde{u}_p - \tilde{u}_p), \nabla\tilde{v})_{0,K} \\ &= \sum_{K \in \mathcal{T}_n} (\boldsymbol{\sigma}_p^\Delta, \nabla\tilde{v})_{0,K} + \sum_{K \in \mathcal{T}_n} (\nabla(\tilde{\Pi}_p^\nabla\tilde{u}_p - \tilde{u}_p), \nabla\tilde{v})_{0,K}. \end{aligned}$$

The assertion follows picking $\tilde{v} = \tilde{u} - \tilde{u}_p$, and using (13) and (16). \square

Next, we investigate the efficiency of the error estimator η_{loc} in (29). We point out that the efficiency is proven up to the presence of a higher order converging term.

Theorem 4.4. *The error estimator η_{loc} in (29) is efficient, i.e., given \tilde{u} and \tilde{u}_p the primal solutions to (2) and (14), and σ_p^Δ as in (30), the following bound is valid:*

$$\sum_{\nu \in \mathcal{V}_n} \|\sigma_p^\Delta\|_{a_p^{\omega_\nu}}^2 \leq (1 + \alpha^*) \left[|\tilde{u} - \tilde{u}_p|_{1, \mathcal{T}_n}^2 + |\tilde{u} - \tilde{\Pi}_p^\nabla \tilde{u}|_{1, \mathcal{T}_n}^2 \right], \quad (31)$$

where $\tilde{\alpha}^*$ and α^* are stability constants appearing in (13) and (16).

Proof. The proof follows along the same lines as of Theorem 4.2. Moreover, we only focus on the case of ν internal vertex. Boundary vertices yield to a similar analysis. In overall, each local flux σ_p^ν minimizes the $a_p^{\omega_\nu}$ norm amongst all functions in a discrete kernel. Therefore, the proof boils down to find a discrete flux $\tau_p^{\Delta, \nu}$ that we can estimate from above by means of the primal error. Such $\tau_p^{\Delta, \nu}$ is the virtual element interpolant of $\tau^{\Delta, \nu}$, which is defined as ∇w^ν , where, for all $K \in \mathcal{T}_n$

$$\begin{cases} \Delta w^\nu = r_\nu^K (= \tilde{\Pi}_1^\nabla \tilde{\varphi}_\nu (f + \Delta \tilde{\Pi}_p^\nabla \tilde{u}_p)) & \text{in } K \\ \mathbf{n}_K \cdot \nabla w^\nu = \tilde{\varphi}_\nu (\mathbf{n}_K \cdot (\nabla \tilde{\Pi}_p^\nabla \tilde{u}_p - \nabla \tilde{u})) - c_\nu^{e, K} & \forall e \in \mathcal{E}^K \\ \int_K w^\nu = 0, \end{cases}$$

where $c_\nu^{e, K}$ is zero on all edges of K except the two having endpoint ν . In particular, $c_\nu^{e, K}$ is always zero on all the boundary edges of ω_ν . The values of $c_\nu^{e, K}$ are to be sought such that (i) the jump of the Neumann traces across e are zero; (ii) the above problem admits compatibility conditions and thence is well posed.

Flicking through all the N_ν elements abutting ν , we have $2 N_\nu$ (each internal edge of ω_ν is shared by two elements) constants to fix by means of N_ν conditions given by the zero jumps and N_ν conditions given by the fact that we want to have compatibility conditions for the above Laplace-Neumann problem.

Having a closer look, simple computations give that the compatibility conditions are as follows: for all $K \in \mathcal{T}_n(\omega_\nu)$ and given e_1 and e_2 the two edges in \mathcal{E}^K with endpoint ν , we have that

$$\begin{aligned} \sum_{j=1}^2 |e_j| c_\nu^{e_j, K} &= (\tilde{\varphi}_\nu, \mathbf{n}_K \cdot (\nabla \tilde{\Pi}_p^\nabla \tilde{u}_p - \nabla \tilde{u}))_{0, \partial K} - (\tilde{\Pi}_1^\nabla \tilde{\varphi}_\nu, -\Delta \tilde{u} + \Delta \tilde{\Pi}_p^\nabla \tilde{u}_p)_{0, K} \\ &= (\tilde{\varphi}_\nu, \mathbf{n}_K \cdot (\nabla \tilde{\Pi}_p^\nabla \tilde{u}_p - \nabla \tilde{u}))_{0, \partial K} - (\tilde{\Pi}_1^\nabla \tilde{\varphi}_\nu, \mathbf{n}_K \cdot (\nabla \tilde{\Pi}_p^\nabla \tilde{u}_p - \nabla \tilde{u}))_{0, \partial K} \\ &\quad - (\nabla \tilde{\Pi}_1^\nabla \tilde{\varphi}_\nu, \nabla (\tilde{u} - \tilde{\Pi}_p^\nabla \tilde{u}_p))_{0, K}. \end{aligned}$$

Importantly, the properties of the partition of unity entails that

$$\sum_{\nu \in \mathcal{V}^K} \sum_{j=1}^2 |e_j| c_\nu^{e_j} = 0. \quad (32)$$

To fully fix the $c_\nu^{e, K}$ constants, we simply impose zero jump conditions across edges of the normal components of the gradients.

Further, observe that $\tau_p^{\Delta, \nu}$ belongs to $\mathbf{Z}_p(\omega_\nu)$, where $\mathbf{Z}_p(\omega_\nu)$ is the obvious local counterpart of (25).

We are left to show the upper bound on the sum of the $\|\tau^{\Delta, \nu}\|_{a_p}$ on an element $K \in \mathcal{T}_n$. For each $\nu \in \mathcal{V}^K$, we have

$$\begin{aligned} \|\tau^{\Delta, \nu}\|_{0, K}^2 &= (\tau^{\Delta, \nu}, \nabla w^\nu)_{0, K} = -(\text{div } \tau^{\Delta, \nu}, w^\nu)_{0, K} + (\mathbf{n}_K \cdot \tau^{\Delta, \nu}, w^\nu)_{0, \partial K} \\ &= -(\tilde{\Pi}_1^\nabla \tilde{\varphi}_\nu (f + \Delta \tilde{\Pi}_p^\nabla \tilde{u}_p), w^\nu)_{0, K} + (\tilde{\varphi}_\nu (\mathbf{n}_K \cdot (\nabla \tilde{\Pi}_p^\nabla \tilde{u}_p - \nabla \tilde{u})) - c_\nu, w^\nu)_{0, \partial K}. \end{aligned}$$

Summing up over all the vertices of K and using (32), we deduce

$$\sum_{\nu \in \mathcal{V}^K} \|\tau^{\Delta, \nu}\|_{0, K}^2 = -(f + \Delta \tilde{\Pi}_p^\nabla \tilde{u}_p, w^\nu)_{0, K} + (\mathbf{n}_K \cdot (\nabla \tilde{\Pi}_p^\nabla \tilde{u}_p - \nabla \tilde{u}), w^\nu)_{0, \partial K}.$$

To conclude, it suffices to proceed exactly as in the proof of Theorem 4.2. \square

5. NUMERICAL RESULTS

Here, we numerically validate the reliability and efficiency of the error estimators η and η_{loc} in (23) and (29).

Since the primal formulation error $|\tilde{u} - \tilde{u}_p|_{1,\Omega}$ is not computable, we rather consider the projected error

$$|\tilde{u} - \tilde{\Pi}_p^\nabla \tilde{u}_p|_{1,\mathcal{T}_n}. \quad (33)$$

Introduce the L-shaped domain

$$\Omega := (-1, 1)^2 \setminus (-1, 0] \times (-1, 0].$$

Given (r, θ) the polar coordinates at $(0, 0)$, we consider the test case

$$u(r, \theta) = r^{\frac{2}{3}} \sin\left(\frac{2}{3}\theta\right) \quad \text{in } \Omega. \quad (34)$$

The remainder of this section is organized as follows. In Section 5.1, we numerically investigate the efficiency and p -robustness of the proposed error estimators by observing the performance of the efficiency index. After presenting the adaptive algorithm and the concept of hp -adaptive mesh refinements in Section 5.1, we compare the performance of the h - and hp -adaptive methods in Section 5.3.

5.1. Efficiency index. Introduce the global and local efficiency indices

$$I^2 := \frac{\eta^2}{|\tilde{u} - \tilde{\Pi}_p^\nabla \tilde{u}_p|_{1,\mathcal{T}_n}}, \quad I_{\text{loc}}^2 := \frac{\eta_{\text{loc}}^2}{|\tilde{u} - \tilde{\Pi}_p^\nabla \tilde{u}_p|_{1,\mathcal{T}_n}}. \quad (35)$$

We run a uniform p -version of the virtual element method on a Cartesian mesh of 48 elements for the test case with exact solution u , compute the corresponding global and localized efficiency indices in (35), and display them in Figure 1.

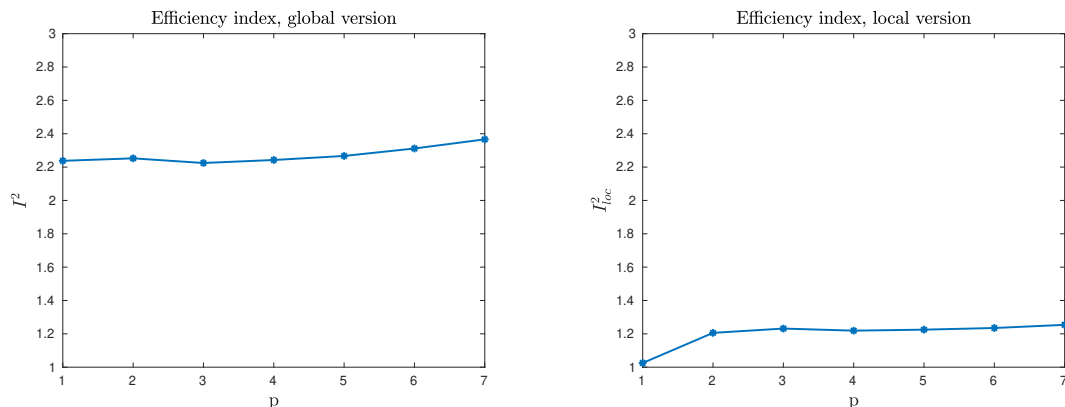


Figure 1. Behaviour of the efficiency indices in (35) for the p -version of the method. *Left panel:* I . *Right panel:* I_{loc} .

From Figure 1, we observe that both the efficiency indices remain close to fix values: the global one approximately to 2.3; the local one approximately to 1.3. This confirms the p -robustness of the proposed error estimator. Even more interestingly, the stability constants appearing in the efficiency estimates (24) and (31) seem to be p -independent in practice.

5.2. The adaptive algorithm and hp -adaptive mesh refinements. A standard adaptive algorithm reads

$$\text{SOLVE} \implies \text{ESTIMATE} \implies \text{MARK} \implies \text{REFINE}.$$

Since the solving and estimation parts are clear, we provide few details for the marking and refining steps.

As for the marking strategy, we follow [11]: we compute the average of the local error estimators

$$\eta_{\text{average}} := \frac{1}{\text{card}(\mathcal{T}_n)} \sum_{K \in \mathcal{T}_n} \eta_K,$$

where η_K denotes any local error estimator on the element K , and mark the elements whose error estimator is larger than $\theta \eta_{\text{average}}$ for a given positive parameter θ . In the numerical experiments below, we pick $\theta = 0.75$.

Further, we follow the hp -refinement strategy of Melenk and Wohlmuth [11] to choose whether performing h - or p -refinements. We refer to [7, Section 4], for more details, notably on the choice of refining parameters, as well as on how the elements are refined.

5.3. The h - and hp -adaptive algorithm. Here, based on the adaptive algorithm discussed in Section 5.2, we investigate the performance of the h - and hp -versions of the VEM upon using the corresponding mesh refinements. We adapt meshes and spaces using both the global (23) and localized (29) error estimators.

In Figure 2, we plot the computable error (33) for the h -version with $p = 1, 2$, and 3, as well as the hp -version of the method for the test case u . As a starting mesh, we employ a coarse uniform Cartesian mesh consisting of 12 squares.

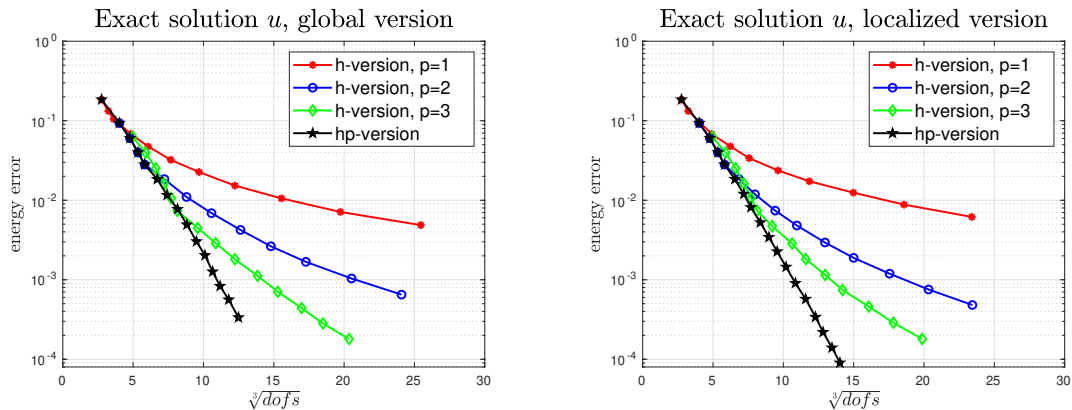


Figure 2. The computable error (33) for the h -version with $p = 1, 2$, and 3, as well as the hp -version of the method for the test case with exact solution in (34). The starting mesh is a uniform Cartesian mesh made of 12 squares. h - and hp -refinements using (*left panel*:) the global error estimator (23); (*right panel*:) the local error estimator (29).

For both versions, we observe the expected rate of convergence: algebraic convergence for the h -version; exponential convergence for the hp -version.

6. CONCLUSIONS

We designed two reliable and efficient error estimators for the virtual element method based on global and local flux reconstruction. The corresponding mixed problem are hybridized. This allows us to overcome the limitation of our previous approach hinging upon employing a standard mixed formulation [7]. The theoretical results are validated by numerical experiments. As *per se* interesting, pivot results, we highlight the existence of a stabilization term for mixed virtual elements, with stability constants having explicit dependence on the degree of accuracy of the method, and the well posedness of the hybridized mixed VEM for diffusion problems.

7. ACKNOWLEDGEMENTS

L. M. acknowledges support from the Austrian Science Fund (FWF) project P33477.

APPENDIX A. STABILIZATIONS FOR MIXED VIRTUAL ELEMENTS WITH EXPLICIT BOUNDS IN TERMS OF THE DEGREE OF ACCURACY

Here, we introduce an explicit stabilization $S^K(\cdot, \cdot)$ as in (15) and prove the two bounds in (16) with explicit dependence in terms of the degree of accuracy p . To the aim, we extend the strategies undertaken in [2].

We define the stabilizing bilinear form

$$S^K(\boldsymbol{\sigma}_p, \boldsymbol{\tau}_p) := (\mathbf{n}_K \cdot \boldsymbol{\sigma}_p, \mathbf{n}_K \cdot \boldsymbol{\tau}_p)_{-\frac{1}{2}, \partial K} + h_K^2 (\operatorname{div} \boldsymbol{\sigma}_p, \operatorname{div} \boldsymbol{\tau}_p)_{0, K} \quad \forall \boldsymbol{\sigma}_p, \boldsymbol{\tau}_p \in \ker(\boldsymbol{\Pi}_p^0) \cap \boldsymbol{\Sigma}_p(K). \quad (36)$$

Proposition A.1. *For all $K \in \mathcal{T}_n$, the stabilization $S^K(\cdot, \cdot)$ defined in (36) satisfies the two bounds in (16) with*

$$\alpha_* \gtrsim p^{-8}, \quad \alpha^* \lesssim p^4. \quad (37)$$

Proof. Without loss of generality, we assume that $h_K = 1$. The general statement follows from a scaling argument.

Given $\boldsymbol{\tau}_p \in \ker(\boldsymbol{\Pi}_p^0) \cap \boldsymbol{\Sigma}_p(K)$, we consider the following Helmholtz-type decomposition of $\boldsymbol{\tau}_p$:

$$\boldsymbol{\tau}_p := \nabla \psi + \mathbf{curl} \rho. \quad (38)$$

We require the two functions ψ and ρ to satisfy

$$\begin{cases} \Delta \psi = \operatorname{div} \boldsymbol{\tau}_p & \text{in } K \\ \mathbf{n}_K \cdot \nabla \psi = \mathbf{n}_K \cdot \boldsymbol{\tau}_p & \text{on } \partial K \\ \int_K \psi = 0 \end{cases} \quad (39)$$

and

$$\begin{cases} (\Delta \rho) \operatorname{rot} \mathbf{curl} \rho = \operatorname{rot} \boldsymbol{\tau}_p & \text{in } K \\ \rho = 0 & \text{on } \partial K. \end{cases} \quad (40)$$

It is apparent the $L^2(K)$ orthogonality of $\nabla \psi$ and $\mathbf{curl} \rho$, whence the following identity follows:

$$\|\boldsymbol{\tau}_p\|_{0, K}^2 = \|\mathbf{curl} \rho\|_{0, K}^2 + |\psi|_{1, K}^2. \quad (41)$$

In order to derive the estimates on α_* , we have to show upper bounds for the two terms on the right-hand side of (41). We begin with that involving ψ using the trace and Poincaré inequalities:

$$\begin{aligned} |\psi|_{1, K}^2 &= - \int_K (\Delta \psi) \psi + \int_{\partial K} (\mathbf{n}_K \cdot \nabla \psi) \psi \stackrel{(39)}{=} - \int_K \operatorname{div} \boldsymbol{\tau}_p \psi + \int_{\partial K} (\mathbf{n}_K \cdot \nabla \psi) \psi \\ &\lesssim \|\operatorname{div} \boldsymbol{\tau}_p\|_{0, K} |\psi|_{1, K} + \|\mathbf{n}_K \cdot \boldsymbol{\tau}_p\|_{-\frac{1}{2}, \partial K} |\psi|_{1, K}. \end{aligned} \quad (42)$$

Thus, we are left with proving the bound on the term involving ρ . To the aim, we write

$$\|\mathbf{curl} \rho\|_{0, K}^2 = \int_K \mathbf{curl} \rho \cdot \mathbf{curl} \rho = \int_K \rho (\operatorname{rot} \mathbf{curl} \rho) \stackrel{(40)}{=} \int_K \rho (\operatorname{rot} \boldsymbol{\tau}_p).$$

We recall the 2D version of [10, Lemma 2.1]: there exists a stable polynomial inverse operator \mathcal{K} of the rot operator. More precisely, for any $q_{p-1} \in \mathbb{P}_{p-1}(K)$ there exists $\mathbf{q}_p \in [\mathbb{P}_p(K)]^2$ such that

$$\mathbf{q}_p = \mathcal{K} q_{p-1}, \quad \operatorname{rot} \mathbf{q}_p = q_{p-1}, \quad \|\mathcal{K} q_{p-1}\|_{0, K} = \|\mathbf{q}_p\|_{0, K} \lesssim \|\operatorname{rot} \mathbf{q}_p\|_{0, K} = \|q_{p-1}\|_{0, K}. \quad (43)$$

The hidden constant depends only on the shape and size of K . Since $\operatorname{rot} \boldsymbol{\tau}_p \in \mathbb{P}_{p-1}(K)$, there exists $\mathbf{q}_p \in [\mathbb{P}_p(K)]^2$ satisfying (43) with $q_{p-1} = \operatorname{rot} \boldsymbol{\tau}_p$.

In light of (43), we can write

$$\|\mathbf{curl} \rho\|_{0, K}^2 = \int_K \rho (\operatorname{rot} \mathbf{q}_p).$$

We deduce

$$\|\mathbf{curl} \rho\|_{0, K}^2 \stackrel{(40)}{=} \int_K (\mathbf{curl} \rho) \cdot \mathbf{q}_p \stackrel{(38)}{=} \int_K (\boldsymbol{\tau}_p - \nabla \psi) \cdot \mathbf{q}_p.$$

Recalling that $\boldsymbol{\tau}_p$ belongs to $\ker(\boldsymbol{\Pi}_p^0)$, we can write

$$\|\mathbf{curl} \rho\|_{0, K}^2 = - \int_K \nabla \psi \cdot \mathbf{q}_p \leq |\psi|_{1, K} \|\mathbf{q}_p\|_{0, K} \stackrel{(43)}{\lesssim} |\psi|_{1, K} \|\operatorname{rot} \mathbf{q}_p\|_{0, K}. \quad (44)$$

We focus on the last term on the right-hand side. To this aim, recall the following inverse estimate on polygons, which trivially follows from [13, Propositions 3.37 and 3.46]: given b_K the standard piecewise cubic bubble over a shape-regular triangulation of K satisfying $\|b_K\|_{\infty,K} = 1$,

$$\|q_p\|_{0,K} \lesssim p \|b_K^{\frac{1}{2}} q_p\|_{0,K} \quad \forall q_p \in \mathbb{P}_p(K). \quad (45)$$

We have

$$\begin{aligned} \|\operatorname{rot} \mathbf{q}_p\|_{0,K}^2 &\stackrel{(40),(43)}{=} \|\operatorname{rot} \mathbf{curl} \rho\|_{0,K}^2 \stackrel{(45)}{\lesssim} p^2 \|b_K^{\frac{1}{2}} \operatorname{rot} \mathbf{curl} \rho\|_{0,K}^2 = p^2 \int_K (b_K \operatorname{rot} \mathbf{curl} \rho) \operatorname{rot} \mathbf{curl} \rho \\ &= p^2 \int_K \mathbf{curl}(b_K \operatorname{rot} \mathbf{curl} \rho) \mathbf{curl} \rho \leq p^2 \|\mathbf{curl}(b_K \operatorname{rot} \mathbf{curl} \rho)\|_{0,K} \|\mathbf{curl} \rho\|_{0,K}. \end{aligned} \quad (46)$$

Recall the standard polynomial inverse inequality on polygons, see, e.g., [5, Theorem 5]:

$$\|q_p\|_{0,K} \lesssim p^2 \|q_p\|_{-1,K}. \quad (47)$$

The inverse inequality (47) remains valid for vector valued polynomials. We deduce that

$$\begin{aligned} \|\mathbf{curl}(b_K \operatorname{rot} \mathbf{curl} \rho)\|_{0,K} &\lesssim p^2 \sup_{\mathbf{v} \in [H_0^1(K)]^2} \frac{(\mathbf{curl}(b_K \operatorname{rot} \mathbf{curl} \rho), \mathbf{v})_{0,K}}{|\mathbf{v}|_{1,K}} \\ &= p^2 \sup_{\mathbf{v} \in [H_0^1(K)]^2} \frac{(b_K \operatorname{rot} \mathbf{curl} \rho, \operatorname{rot} \mathbf{v})_{0,K}}{|\mathbf{v}|_{1,K}} \lesssim p^2 \|\operatorname{rot} \mathbf{curl} \rho\|_{0,K}. \end{aligned} \quad (48)$$

Using (46) and the above inverse estimate, we arrive at

$$\|\operatorname{rot} \mathbf{q}_p\|_{0,K}^2 \lesssim p^4 \|\operatorname{rot} \mathbf{curl} \rho\|_{0,K} \|\mathbf{curl} \rho\|_{0,K} = p^4 \|\operatorname{rot} \mathbf{q}_p\|_{0,K} \|\mathbf{curl} \rho\|_{0,K}.$$

Inserting this bound in (44) entails

$$\|\mathbf{curl} \rho\|_{0,K} \lesssim p^4 |\psi|_{1,K}.$$

Combining the above estimate with (42) yields the desired bound on α_* .

As for the bound on α^* , we refer to [7, Proposition 2.7] for full details. Here, we only sketch the proof. We need to estimate from above the two terms on the right-hand side of (36). As for the boundary one, we apply a div trace inequality, see, e.g., [12]:

$$\|\mathbf{n}_K \cdot \boldsymbol{\tau}_p\|_{-\frac{1}{2}, \partial K} \lesssim \|\boldsymbol{\tau}_p\|_{0,K} + \|\operatorname{div} \boldsymbol{\tau}_p\|_{0,K}.$$

Therefore, it suffices to estimate the divergence term. This can be done via an inverse inequality as detailed in the proof of [7, Proposition 2.7], which can be proven as in (48):

$$\|\operatorname{div} \boldsymbol{\tau}_p\|_{0,K} \lesssim p^2 \|\boldsymbol{\tau}_p\|_{0,K}.$$

The assertion follows. \square

Remark 1. From the proof of Proposition A.1, it is immediate to check the bound on α^* in (37) is valid not only for functions in $\ker(\boldsymbol{\Pi}^0) \cap \boldsymbol{\Sigma}_p(K)$, but for all functions $\boldsymbol{\tau} \in H(\operatorname{div}, K) \cap H(\operatorname{rot}, K)$ such that $\operatorname{div} \boldsymbol{\tau}$ belongs to $\mathbb{P}_p(K)$.

In practical computations, the boundary contribution in (36) can be substituted by

$$h_K (\mathbf{n}_K \cdot \boldsymbol{\sigma}_p, \mathbf{n}_K \cdot \boldsymbol{\tau}_p)_{0, \partial K}.$$

In this case, it is possible to check that the bounds on the stability constants become

$$\alpha_* \gtrsim p^{-8}, \quad \alpha^* \lesssim p^6.$$

REFERENCES

- [1] D. N. Arnold and F. Brezzi. Mixed and nonconforming finite element methods: implementation, postprocessing and error estimates. *ESAIM Math. Model. Numer. Anal.*, 19(1):7–32, 1985.
- [2] L. Beirão da Veiga and L. Mascotto. Interpolation and stability properties of low order face and edge virtual element spaces. <https://arxiv.org/abs/2011.12834>, 2020.
- [3] L. Beirão da Veiga, F. Brezzi, A. Cangiani, G. Manzini, L.D. Marini, and A. Russo. Basic principles of virtual element methods. *Math. Models Methods Appl. Sci.*, 23(01):199–214, 2013.
- [4] L. Beirão da Veiga, F. Brezzi, L. D. Marini, and A. Russo. Mixed virtual element methods for general second order elliptic problems on polygonal meshes. *ESAIM Math. Model. Numer. Anal.*, 50(3):727–747, 2016.
- [5] L. Beirão da Veiga, A. Chernov, L. Mascotto, and A. Russo. Exponential convergence of the *hp* virtual element method with corner singularity. *Numer. Math.*, 138(3):581–613, 2018.
- [6] D. Braess, V. Pillwein, and J. Schöberl. Equilibrated residual error estimates are *p*-robust. *Comput. Methods Appl. Mech. Engrg.*, 198(13-14):1189–1197, 2009.
- [7] F. Dassi, J. Gedicke, and L. Mascotto. Adaptive virtual elements with equilibrated fluxes. <https://arxiv.org/abs/2004.11220>, 2020.
- [8] F. Dassi, C. Lovadina, and M. Visinoni. Hybridization of the virtual element method for linear elasticity problems. <http://arxiv.org/abs/2103.01164>, 2021.
- [9] A. Ern and M. Vohralík. Polynomial-degree-robust a posteriori estimates in a unified setting for conforming, nonconforming, discontinuous Galerkin, and mixed discretizations. *SIAM J. Numer. Anal.*, 53(2):1058–1081, 2015.
- [10] J. Gopalakrishnan and L. F. Demkowicz. Quasioptimality of some spectral mixed methods. *J. Comput. Appl. Math.*, 167(1):163–182, 2004.
- [11] J. M. Melenk and B. I. Wohlmuth. On residual-based a posteriori error estimation in *hp*-FEM. *Adv. Comput. Math.*, 15(1-4):311–331, 2001.
- [12] P. Monk. *Finite Element Methods for Maxwell's Equations*. Oxford University Press, 2003.
- [13] R. Verfürth. *A posteriori error estimation techniques for finite element methods*. OUP Oxford, 2013.

(F. Dassi) DIP. DI MATEMATICA E APPLICAZIONI, UNIVERSITÀ DEGLI STUDI DI MILANO-BICOCCA, ITALY
Email address: franco.dassi@unimib.it

(J. Gedicke) INSTITUT FÜR NUMERISCHE SIMULATION, UNIVERSITÄT BONN, 53115 BONN
Email address: gedicke@ins.uni-bonn.de

(L. Mascotto) FAKULTÄT FÜR MATHEMATIK, UNIVERSITÄT WIEN, 1090 VIENNA, AUSTRIA
Email address: lorenzo.mascotto@univie.ac.at